PHYSICAL REVIEW B **80**, 041312(R) (2009)

Microphotoluminescence studies of tunable wurtzite $InAs_{0.85}P_{0.15}$ quantum dots embedded in wurtzite InP nanowires

Niklas Sköld,[1] Mats-Erik Pistol,[1] Kimberly A. Dick,[1] Craig Pryor,[2] Jakob B. Wagner,[3] Lisa S. Karlsson,[3] and Lars Samuelson[1]
[1]*Solid State Physics/The Nanometer Structure Consortium, Lund University, P.O. Box 118, S-221 00 Lund, Sweden*
[2]*Department of Physics and Astronomy, University of Iowa, Iowa City, Iowa 52242, USA*
[3]*Polymer and Materials Chemistry/The Nanometer Structure Consortium, P.O. Box 124, S-221 00 Lund, Sweden*
(Received 25 May 2009; published 24 July 2009)

We have investigated the effects of strong confinement in wurtzite $InAs_{0.85}P_{0.15}$ quantum dots embedded in wurtzite InP nanowires using microphotoluminescence spectroscopy. Strain-dependent $\mathbf{k}\cdot\mathbf{p}$ calculations were used to model the quantum dots, and it was found that the electron effective mass was increased by a factor of 2 and the band gap was increased by 190 meV compared to equivalent quantum dots in the zinc-blende polytype. Measurements indicate that there is a relaxation bottleneck giving rise to an anomalous state filling behavior.

DOI: 10.1103/PhysRevB.80.041312 PACS number(s): 78.67.Hc, 78.67.Lt, 81.07.Ta, 81.07.Vb

Semiconductor quantum dots (QDs) are interesting from a fundamental as well as a technological point of view due to their quantized size-dependent energy spectrum. Controlling the size, shape, and density of these QDs is however a difficult task. The most studied epitaxially grown QDs are self-assembled, i.e., grown by island nucleation in the Stranski-Krastanow growth mode. The size, shape, and density of self-assembled QDs can to some extent be controlled by growth parameters such as temperature and growth time,[1] but in the end it is a spontaneous strain induced process and controlling all properties independently is problematic. QDs in nanowires have in contrast shown great potential as a highly controllable system. The diameter, height, and density of the QDs are defined by the nanowire diameter, the growth time, and the nanowire density, respectively, and can be chosen almost arbitrarily. Furthermore, single nanowire QDs can easily be electrically contacted,[2] and since they are not embedded in a high refractive index substrate, the light extraction efficiency increases significantly.[3] Optical studies on QDs in nanowires have shown sharp lines[4–7] and antibunched photon emission,[4] which is characteristic of zero-dimensional systems. The emission has, however, generally been tuned by the material composition rather than the QD size, indicating that confinement effects are still quite weak. In this work we present microphotoluminescence (micro-PL) spectroscopy studies of QDs in nanowires with diameters as small as 9 nm, demonstrating strong confinement effects by tuning emission energies, energy-level splittings, and biexciton binding energies using only the size of the QDs.

The nanowires were grown by low-pressure metalorganic vapor phase epitaxy (MOVPE) on (111)B InP substrates using size selected Au aerosols as seed particles. After aerosol deposition the samples were placed in the MOVPE system on a gas foil rotated graphite disk susceptor heated by halogen lamps. The substrates were first annealed at 600 °C for 10 min in phosphine (PH_3) containing ambient to remove surface oxide after which the temperature was ramped down to the growth temperature 420 °C. InP nanowires were grown using trimethyl-indium (TMI) and PH_3 while InAs nanowires were grown with TMI and arsine (AsH_3). Both InAs and InP showed a growth rate proportional to $1/d$, where d is the nanowire diameter, for wires with a diameter larger than the Gibbs-Thomson critical diameter. This is in agreement with other studies.[8–10] For InAs growth an onset of the Gibbs-Thomson effect was observed at $d \approx 9$ nm (Ref. 11) leading to a decrease in the supersaturation of the Au particle and a decreasing growth rate for thinner wires.[8,10]

The QD heterostructures were grown in InP nanowires by switching from an TMI-PH_3 ambient to an AsH_3 ambient for 5 s. Fröberg *et al.*[12] recently found that the In content of the seed particle is higher in PH_3 ambient than in AsH_3 ambient and that short InAs segments can be grown from In stored in the Au particle only, with no TMI entering the reactor cell. By switching from a TMI-PH_3 ambient to AsH_3 ambient for a few seconds the excess In is expelled, forming an InAs QD with well defined height. As the volume of excess In stored in the Au is proportional to the volume of the seed particle ($\sim d^3$) and the growth interface area is defined by the base of the hemispherical seed particle ($\sim d^2$), the length of the InAs segment grown from stored In can be expected to scale linearly with the nanowire diameter ($\sim d$). For the QDs studied with varying d this results in a QD height, $h = C \cdot d$. Where C is a constant related to the difference in the In content of the seed particle in TMI-PH_3 and AsH_3 ambient, respectively. It has here been assumed that C is independent of the Au particle size. This assumption is valid as long as the In content in the particle is size independent; i.e., the particle is large enough that the Gibbs-Thomson effect can be neglected and the supersaturation is independent of size, which is the case for $d \geq 9$ nm.

Nanowires with diameters in the range of 9–32 nm were produced, and dimensions and compositions of the QD heterostructures were measured using high-angle annular dark field scanning transmission electron microscopy (HAADF-STEM) and x-ray energy dispersive spectrometry (XEDS). For thin nanowires the material contrast was weak in the HAADF-STEM images and XEDS measurements were not feasible due to beam damage. The analysis of the QDs is therefore based on measurements on wires with diameters of 16 and 32 nm. Figure 1 shows a HAADF-STEM image of a nanowire, 16 nm in diameter, with five QDs marked with arrows. The QD closest to the top was grown from In stored

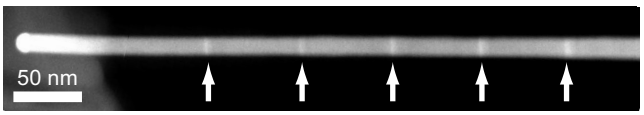

FIG. 1. HAADF-STEM image of five $InAs_{0.85}P_{0.15}$ QDs with different heights in an InP nanowire with 16 nm diameter. The bright signal at the top of the wire (to the left in the image) comes from the carbon film on which the nanowire tip is resting.

in the Au particle by switching on AsH_3 for 5 s and the rest of the QDs, from left to right, were grown with an ambient of both AsH_3 and TMI for 1, 2, 5, and 10 s, respectively. The height of the QDs grown from stored In only was determined to be $h=0.35d$, as measured in the HAADF-STEM images. XEDS point measurements showed that the composition of the QDs was not pure InAs but $InAs_{0.85}P_{0.15}$, probably due to memory effects in the reactor cell. From fast Fourier transforms of high-resolution images it was found that both the $InAs_{0.85}P_{0.15}$ QDs and the InP nanowires had a wurtzite (WZ) crystalline structure with the nanowire axis in the [0001] direction as is common for thin nanowires.[13,14] Stacking faults with a density on the order of 1 stacking fault per 10 nm was furthermore observed as well as a few zinc-blende (ZB) segments; these were however typically not larger than a few nm.

Micro-PL spectroscopy was performed on individual nanowires, containing a single QD with dimensions $9<d<22$ nm and $h=0.35d$. An InP shell, 14 nm thick at the position of the QD, was used for surface passivation to enhance the quantum efficiency. The nanowires were deposited on Si substrates with patterned Au surfaces, and the samples were then mounted in a cold finger cryostat and cooled to 7 K. As excitation source a frequency doubled yttrium aluminum garnet laser emitting at 532 nm was used. The nanowire QD emission was collected with a microscope and dispersed by a spectrometer onto a liquid-N_2-cooled HgCdTe camera. The QD spectrum generally consisted of a single exciton (X) line at low excitation power density. As the excitation power density was increased a biexciton (X_2) line appeared as the exciton line diminished in intensity. The biexciton line was subsequently followed by the triexciton (X_3) line together with a broader feature at higher energies coming from electrons and holes in the first-excited-state recombining. Figure 2(a) shows the excitation power-density dependence of a QD with 11 nm diameter and an estimated height of 3.9 nm (all spectra are normalized). The exciton linewidths varied from 300 μeV to a few meV, possibly affected by the QDs close proximity to the surface. For dots without an InP shell no QD luminescence could be observed illustrating the importance of surface passivation. Wires with a 14 nm shell however showed effects of aging with linewidth broadening after being stored in air for a time period of one month, a problem that could possibly be reduced with a thicker shell. The effect of decreasing QD size on the spectrum is illustrated in Fig. 2(b), which shows the normalized spectra of three QDs with diameters 11, 16, and 22 nm. For each QD the spectra at three different excitation power densities are presented, the bottom trace shows the single X line, the middle trace shows both the X and X_2 lines, while the top trace shows the excited states. Figure 2(b) illustrates the general trend of blueshifted energy spectra, increasing level splittings, and increasing X_2-X splitting (as a consequence of increasing interactions between the carriers due to stronger confinement) with decreasing QD size. The largest QD, represented by the top three black traces, is emitting at a wavelength of 1300 nm,

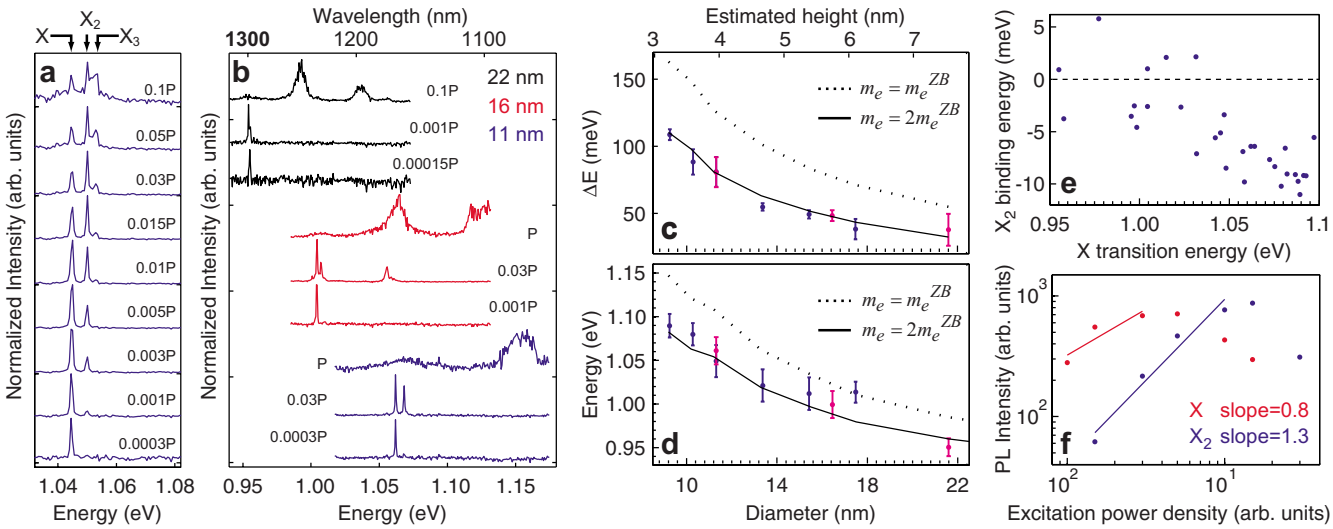

FIG. 2. (Color online) (a) Micro-PL spectra at different excitation power densities for a single $InAs_{0.85}P_{0.15}$ QD in a InP nanowire showing the X, X_2, and X_3 emissions. (b) Size dependence of the QD spectrum for three dots of different sizes at three different excitation power densities. The largest QD is emitting at the telecommunication wavelength of 1300 nm, and the emission blueshifts with decreasing QD size. All spectra were measured at 7 K, $P=800$ W/cm^2. (c) and (d) Energy splitting between the ground state and the first-excited-state transition and exciton transition energy, respectively, vs diameter (d) for QDs with height $h=0.35d$. Dots mark experimental data points, with error bars corresponding to one standard deviation; different colors represent two different growth runs. Calculated transition energies using $m_e=m_e^{ZB}$ (dotted line) and $m_e=2m_e^{ZB}$ (solid line) are blueshifted 190 meV for clarity. (e) X_2 binding energy vs X transition energy. (f) Power dependence of X and X_2 lines.

emphasizing the potential application of these QDs as single-photon emitters at telecommunication wavelengths.

The QDs were modeled by strain-dependent $\mathbf{k}\cdot\mathbf{p}$ calculations and compared to experimental data. The strain was modeled using continuum elasticity theory, and the strain energy was minimized on a $100\times100\times100$ cubic grid using finite difference methods. The resulting strain tensor elements were then used as inputs to a strain dependent six-band $\mathbf{k}\cdot\mathbf{p}$ Hamiltonian. Due to the lack of WZ material parameters for both InAs and InP, ZB material parameters from Ref. 15 were used instead, except for the electron effective mass, which was used as fitting parameter. InAs is expected to have a larger band gap in its WZ polytype compared to the ZB polytype, and as a consequence of the larger band gap the charge-carrier effective masses also increase according to Kane's model.[15] In the calculations the nanowire and QD geometries were approximated as cylinders in the [111] direction. The emission energies of $InAs_{0.85}P_{0.15}$ QDs with dimensions $9<d<22$ nm and $h=0.35d$ surrounded by a 14-nm-thick InP shell were calculated.

A rough estimate of the electron effective mass can be obtained from the splitting between the ground and first-excited state, ΔE, which mainly depends on the split between the electron states. Although the positions of the energy levels depend sensitively on the strain situation, the split between them is quite insensitive to strain since the conduction-band offset is much less sensitive to a change in material parameters than the position of the conduction-band edge. Therefore, the electron effective mass, m_e, can be estimated from the size dependence of ΔE even though the elastic constants and deformation potentials are unknown for the WZ polytype. Figure 2(c) shows ΔE for the measured QDs together with calculated splits for the transition energies using ZB material parameters (dotted line) and with m_e as a fitting parameter, a good fit to the experimental data is achieved with $m_e=2m_e^{ZB}$ (solid line). The increased electron effective mass can be compared to the nitrides where material parameters exist for both the WZ and ZB polytype and the electron effective mass is between 0 and 33% larger for the WZ polytype compared to ZB (InN and GaN respectively).[16] In this respect a 100% increase is unexpectedly large. However, InAs is a small band-gap material and the fractional change in band gap between the ZB and WZ polytypes is quite large (which will be discussed below). This means that the change in electron effective mass should be large as well according to Kane's model. Using the electron effective mass $m_e=2m_e^{ZB}$, as determined from the level splittings, the $\mathbf{k}\cdot\mathbf{p}$ calculations yielded ground-state transition energies approximately 190 meV lower than the experimental energies. Apart from this there is good agreement between calculations and experimental data. Figure 2(d) shows the measured transition energies for the ground state together with the calculated energies for $m_e=2m_e^{ZB}$ (solid line) and $m_e=m_e^{ZB}$ (dotted line); all calculated energies are shifted 190 meV for clarity. The shift in emission energy corresponds to the band-gap offset for WZ $InAs_{0.85}P_{0.15}$ compared to ZB, which therefore from the $m_e=2m_e^{ZB}$ curve can be estimated to be 190 meV. This band-gap increase is in reasonable agreement with the few experimental studies of the band gap of WZ InAs[17,18] where the increase has been reported to be 120 and 150 meV, respectively. The change in band gap is thus rather big when compared to the 420 meV band gap of ZB InAs.[15] It should be noted that our model is quite crude since elastic constants and deformation potentials are not known for the WZ polytype of our material system; nor are the piezoelectric constants known and piezoelectric fields are thus omitted from the calculations. The estimates of the band gap as well as the electron effective mass should be viewed in light of this.

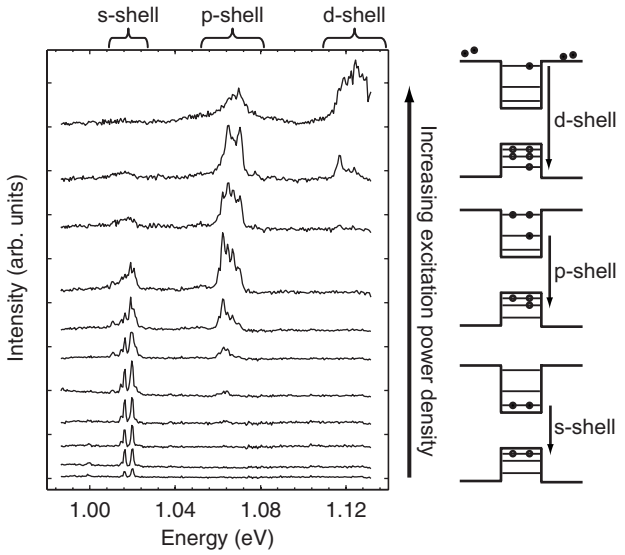

FIG. 3. Power-density dependence of the QD spectrum and schematic of the recombination paths for a QD with slow electron relaxation.

Both negative and positive X_2 binding energies were observed, ranging between −11 and 6 meV (with the biexciton line appearing on the high- and low-energy sides of the exciton line, respectively). Figure 2(e) shows the trend of more negative X_2 binding energies for QDs with stronger confinement. Coulomb, exchange, and correlation interactions depend sensitively on the QD size and shape, which can result in negative binding energies for small QDs if repulsive electron-electron, hole-hole Coulomb interactions dominate over attractive electron-hole interactions. For self-assembled QDs it has been reported that both positive and negative binding energies of exciton complexes occur.[19–21] A similar trend as shown in Fig. 2(e) with increasingly negative X_2 binding energy for stronger confinement has been reported for self-assembled QDs,[20] but the opposite trend has also been observed.[21] It can be expected that the X_2 binding energy can show either trend depending on how the QD geometry and material system affects the overlap of the charge-carrier wave functions.

An anomalous state filling behavior of the nanowire QDs was observed. The X and X_2 intensities generally increased sublinearly and subquadratically, respectively, as shown in Fig. 2(f). This could indicate a slow relaxation process[22] due to a phonon bottleneck. Furthermore, as the excited states appeared in the QD spectrum, the lower lying states did not only saturate but were actually quenched. Figure 3 shows the excitation power dependence of one of the larger QDs ($d=17$ nm) where the ground state and the first two excited

states are visible (here termed the *s*, *p*, and *d* shell in analogy with atomic orbitals). It is possible that the electron relaxation is slower than the hole relaxation due to the larger separation between the electron levels in the presence of a phonon bottleneck.[23] The holes therefore attain their equilibrium configuration before the electrons, and if the electron relaxation time is slower than the recombination time the recombination path will be determined by the highest occupied hole level. When an electron reaches the corresponding level it will recombine and lower lying electron levels are never filled. A schematic illustration of such a process can be seen to the right in Fig. 3. At low excitation power the *s*-shell luminescence is observed, but when the holes start to occupy the *p* shell the *s*-shell luminescence quenches since the electrons never reach the ground state. In analogy the *p*-shell luminescence quenches when the holes start to occupy the *d* shell. The existence of a phonon bottleneck is expected for zero-dimensional quantum systems but generally not observed for self-assembled QDs. It is possible that the reduction in the number of phonon modes in the one-dimensional nanowire structure makes QDs in nanowires more susceptible to such a bottleneck. Furthermore the charge carriers in a self-assembled QD can relax via the Auger process[24] by coupling to the electron-hole plasma in the wetting layer, a relaxation path that does not exist for nanowire QDs as there is no wetting layer.

In conclusion, we have produced WZ $InAs_{0.85}P_{0.15}$ QDs with well-defined dimensions in WZ InP nanowires. Emission energies, energy-level splittings, and biexciton binding energies were tuned by changing the QD size, illustrating the high level of control of the QD spectrum achievable for QDs in nanowires. Fitting experimental data to a strain-dependent $\mathbf{k}\cdot\mathbf{p}$ model with ZB material parameters using the electron effective mass as a fitting parameter yielded a factor of 2 increase in electron effective mass and a band-gap increase of 190 meV compared to equivalent QDs in the ZB polytype. An anomalous state filling behavior of the nanowire QDs was observed, possibly indicating the presence of a phonon bottleneck.

We thank L. E. Fröberg and J. Johansson for valuable discussions. This work was carried out within the Nanometer Structure Consortium in Lund and was supported by the Swedish Foundation for Strategic Research (SSF), the Swedish Research Council (VR), Knut and Alice Wallenberg Foundation, NoE SANDiE (EU Grant No. 500101) and NODE (EU Grant No. 015783).

[1] J. Oshinowo, M. Nishioka, S. Ishida, and Y. Arakawa, Appl. Phys. Lett. **65**, 1421 (1994).
[2] M. T. Björk, C. Thelander, A. E. Hansen, L. E. Jensen, M. W. Larsson, L. Reine Wallenberg, and L. Samuelson, Nano Lett. **4**, 1621 (2004).
[3] J. Zhu and Y. Cui, Small **3**, 1322 (2007).
[4] M. T. Borgström, V. Zwiller, E. Müller, and A. Imamoglu, Nano Lett. **5**, 1439 (2005).
[5] E. D. Minot *et al.*, Nano Lett. **7**, 367 (2007).
[6] M. Tchernycheva, G. E. Cirlin, G. Patriarche, L. Travers, V. Zwiller, U. Perinetti, and J.-C. Harmand, Nano Lett. **7**, 1500 (2007).
[7] M. H. M. van Weert, N. Akopian, U. Perinetti, M. P. van Kouwen, R. E. Algra, M. A. Verheijen, E. P. A. M. Bakkers, L. P. Kouwenhoven, and V. Zwiller, Nano Lett. **9**, 1989 (2009).
[8] J. Johansson, C. P. T. Svensson, T. Mårtensson, L. Samuelson, and W. Seifert, J. Phys. Chem. B **109**, 13567 (2005).
[9] L. Schubert, P. Werner, N. D. Zakharov, G. Gerth, F. M. Kolb, L. Long, U. Gösele, and T. Y. Tan, Appl. Phys. Lett. **84**, 4968 (2004).
[10] L. E. Fröberg, W. Seifert, and J. Johansson, Phys. Rev. B **76**, 153401 (2007).
[11] See EPAPS Document No. E-PRBMDO-80-R26928 for InAs and InP nanowire growth rates as a function of the diameter. The decrease in InAs growth rate for wires with $d<9$ nm is attribued to the Gibbs-Thomson effect. The InAs growth rate is determined from pure InAs nanowires and does not correspond to the growth rate of the quantum dots as the surface diffusion on the nanowire side facets is different for InP and InAs surfaces. For more information on EPAPS, see http://www.aip.org/pubservs/epaps.html.
[12] L. E. Fröberg, B. A. Wacaser, J. B. Wagner, S. Jeppesen, B. J. Ohlsson, K. Deppert, and L. Samuelson, Nano Lett. **8**, 3815 (2008).
[13] P. Caroff, K. A. Dick, J. Johansson, M. E. Messing, K. Deppert, and L. Samuelson, Nat. Nanotechnol. **4**, 50 (2009).
[14] T. Akiyama, K. Sano, K. Nakamura, and T. Ito, Jpn. J. Appl. Phys., Part 2 **45**, L275 (2006).
[15] I. Vurgaftman, J. R. Meyer, and L. R. Ram-Mohan, J. Appl. Phys. **89**, 5815 (2001).
[16] I. Vurgaftman and J. R. Meyer, J. Appl. Phys. **94**, 3675 (2003).
[17] J. Trägårdh, A. I. Persson, J. B. Wagner, D. Hessman, and L. Samuelson, J. Appl. Phys. **101**, 123701 (2007).
[18] Z. Zanolli, M.-E. Pistol, L. E. Fröberg, and L. Samuelson, J. Phys.: Condens. Matter **19**, 295219 (2007).
[19] Ph. Lelong and G. Bastard, Solid State Commun. **98**, 819 (1996).
[20] S. Rodt, R. Heitz, A. Schliwa, R. L. Sellin, F. Guffarth, and D. Bimberg, Phys. Rev. B **68**, 035331 (2003).
[21] J. Persson, M. Holm, C. Pryor, D. Hessman, W. Seifert, L. Samuelson, and M. E. Pistol, Phys. Rev. B **67**, 035320 (2003).
[22] M. Grundmann and D. Bimberg, Phys. Rev. B **55**, 9740 (1997).
[23] *Optics of Quantum Dots and Wires*, edited by G. W. Bryant and G. S. Solomon (Artech House, London, 2005), pp. 38–45.
[24] A. D. Yoffe, Adv. Phys. **50**, 1 (2001).